Substituent Control of the Reductive Nitrosylation of *Wilkinson*'s Catalyst by Diazeniumdiolates

by **Navamoney Arulsamy**, **David Scott Bohle***, and **Blaine Doletski**

Department of Chemistry, University of Wyoming, Laramie, WY 82071-3838 USA

Dedicated to the memory of Professor *Luigi M. Venanzi*

Diazeniumdiolates ($RN(O)NO^-$, R = Et, Et_2N) react in an R-dependent manner with *Wilkinson*'s catalyst to give either a chelated square-planar complex, $Rh(\eta^2\text{-}O_2N_2Et)(PPh_3)_2$, **1**, for R = Et, or with initial chelation followed by reductive nitrosylation to give $Rh(NO)(PPh_3)_3$, in the case of $R = Et_2N$. Methyl iodide oxidatively adds to **1** to give $RhIMe(\eta^2\text{-}O_2N_2Et)(PPh_3)_2$, **2**, as a pair of isomers **a**, major, and **b**, minor. Both **1** and **2a** have been structurally characterized by single-crystal X-ray diffraction.

1. Introduction. – The diazeniumdiolates, $RN(O)NO^-$ [1] are a surprisingly diverse array of compounds, which range from natural products ($R=CH_2CH(NH_2)CO_2H$, alanosine) [2], to organometallic derivatives [$Me_4W((\eta^2\text{-}O_2N_2Me)_2$] [3], to biomedical reagents ($R = R'_2N$, 'nonoates') [1], to analytical reagents (R=Ph, cupferron) [4]. Their reactivity patterns are strongly R-dependent, and vary from attack at addition to either oxygen [5][6] to heterolytic cleavage of the R–N bond to give either R^- and 2 NO [7] or R^+ and $N_2O_2^{2-}$ [8]. All of these reactions are markedly electrophile-dependent, and the factors that control the specific reaction remain poorly understood.

Although (*Z*)-1-phenyldiazen-1-ium-1,2-diolate ($PhN(O)NO^-$) has been extensively used as an analytical tool for the detection of Fe^{II} and Cu^{II}, the coordination chemistry of alkyl and aryl diazeniumdiolates in low-valent Pt-group metal complexes is limited to the synthesis and structural characterization of several Rh^I carbonyl complexes [9–12]. At the outset of this research, we hypothesized that an electron-rich low-valent transition metal might be either reductively nitrosylated by the diazeniumdiolate, to give a nitrosyl complex, or otherwise activate the diazeniumdiolate towards electrophilic attack at nitrogen. To test these possibilities, we have reexamined the Rh^I chemistries of (*Z*)-1-ethyldiazen-1-ium-1,2-diolate and (*Z*)-1,1-diethylaminodiazen-1-ium-1,2-diolate and report the synthesis and characterization of $Rh(\eta^2\text{-}O_2N_2Et)(PPh_3)_2$ (**1**) and its MeI addition product, $RhIMe(\eta^2\text{-}O_2N_2Et)(PPh_3)_2$ (**2a**,**b**). In contrast to diethylaminodiazenium diolate, which reductively nitrosylates the metal center after chelation, the ethyldiazeniumdiolate complexes **1** and **2** undergo neither reductive nitrosylation nor electrophilic *N* alkylation.

2. Results. – *Wilkinson*'s catalyst rapidly reacts with potassium ethyldiazeniumdiolate to give **1**, which can be isolated as an orange crystalline solid in excellent yield (*Scheme 1*). ^{31}P-NMR Spectroscopic data in CD_2Cl_2 show a single temperature-independent eight-line pattern corresponding to a doubled AB quartet, and is

interpreted as being due to two inequivalent nonexchanging triphenylphosphine ligands in a square-planar complex. This geometry was subsequently confirmed by single-crystal X-ray diffraction, below, and its purity confirmed by elemental analysis after recrystallization from CH_2Cl_2/EtOH. In the solid state, differential scanning calorimetry demonstrates that the complex does not undergo any phase transitions or reactions until its irreversible endothermic decomposition at 208°, $\Delta H = +393\ J\ g^{-1}$, and, in solution, the NMR is unchanged when heated in deuterotoluene at 96° for 40 minutes.

Scheme 1

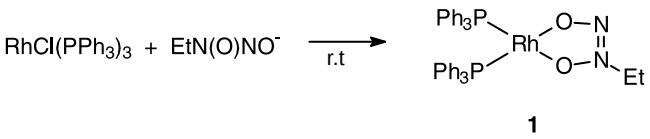

1

In contrast with the stability of **1** is the related complex where a diethylamino is the R substituent. In this case, when $RhCl(PPh_3)_3$ is treated with $[Et_2NH_2]$ $[Et_2NN(O)NO]$ under the same conditions as employed in the preparation of **1**, the product, $Rh(NO)(PPh_3)_3$, results from reductive nitrosylation (*Scheme 2*). When the reaction is followed by ^{31}P-NMR, there is an equally rapid reaction, with the initial product also having an eight-line doubled-AB-quartet spectrum, similar to **1**; the ^{1}H-NMR spectrum has a corresponding single set of new ethyl resonances, which rapidly appears and then disappears on standing (see *Exper. Part*). The spectroscopic equivalence of the ethyl groups, the inequality of the two triphenylphosphines, and the similarity of this complex to **1** suggest that this intermediate has the square-planar structure shown (**A**, *Scheme 2*). Within 30 min, however, this spectrum disappears and is replaced by that corresponding to a mixture of products, the largest component of which is a *doublet* at *ca.* $\delta = 50$ ppm. The IR spectrum of the solids isolated from the solution by addition of hexane and concentration is dominated by a single band at 1610 cm^{-1} (NO). Taken together, these data correspond to the main decomposition product being $Rh(NO)(PPh_3)_3$, based on the comparison of its known spectroscopic properties [13][14].

Scheme 2

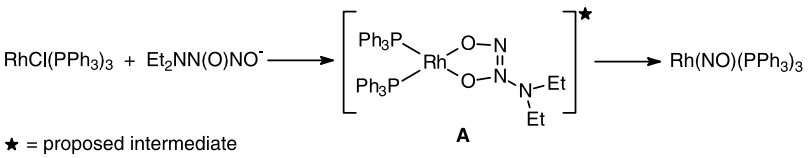

A

Oxidative addition of MeI to **1** gives a mixture of isomers, both of which correspond to metal addition, and are formulated as geometric isomers of $RhIMe(\eta^2\text{-}O_2N_2Et)(PPh_3)_2$ (**2a**,**b**, *Scheme 3*). The ^{31}P-NMR spectra of both products have equivalent triphenylphosphines, suggesting a *trans* geometry of these ligands, and both contain new doubled triplets in the ^{1}H-NMR spectrum. The latter data corresponds to a metal bound Me group coupled to a single ^{103}Rh and two ^{31}P nuclei. Integration of the

related pairs of peaks in the ^{1}H-NMR spectrum give a ratio of 5 : 1 for the two isomers, and **2a** has been shown by single-crystal X-ray diffraction, below, to have the geometry shown in *Scheme 3*, where the metal-bound Me is *trans* to the ON group bearing the ethyl substituent.

Scheme 3

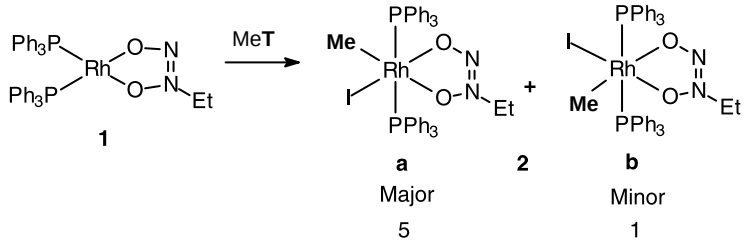

1 **a** **2** **b**

Major Minor

5 1

Compounds **1** and **2a** have been characterized by single-crystal X-ray diffraction. The relevant experimental and metric parameters are collected in *Tables 1* and *2* respectively, with ORTEP views shown in *Figs. 1–3*. For complex **1**, refinement of the diffraction data led to a very clear disorder in the ethyl substituent over two positions, with the CH_2 slightly above and below the plane and the Me twisted in the opposite direction, *Fig. 2*. For complex **2a**, these same ethyldiazeniumdiolate C-atoms refine with significantly higher thermal parameters, also suggesting a certain conformational freedom, although not as pronounced as in **1**. The isomeric mixture of **2** crystallized as a large blocks, and mechanical sorting of several identical crystals to that used in the

Table 1. *Crystallographic Data for* **1** *and* **2a**

	1	**2a**
Empirical formula	$C_{38}H_{35}N_2O_2P_2Rh$	$C_{39}H_{38}IN_2O_2P_2Rh$
Crystal size [mm^3]	$0.65 \times 0.3 \times 0.25$	$0.38 \times 0.20 \times 0.10$
Space group	$P2_1/c$	$P2_1/c$
a [Å]	9.9306(9)	13.538(2)
b [Å]	9.2163(11)	15.177(2)
c [Å]	37.415(4)	18.982(3)
α [°]	90	90
β [°]	95.145(8)	90.231(13)
γ [°]	90	90
V [Å^3]	3410.5(6)	3900.1(11)
Z	4	4
μ [mm^{-1}]	0.630	1.350
ρ_{calcd} [g cm^{-3}]	1.395	1.517
No. of measured refl.	7987	8403
No. of observed refl.	4784	4346
No. of parameters	421	441
S_{gof} on F^2	1.043	1.021
R_1[a]) $[F > 4\sigma(F)]$	0.0341	0.0562
wR_2[b])[c])	0.0785	0.1226

[a]) $R_1 = \Sigma\,||F_o| - |F_c||/\Sigma\,|F_o|$. [b]) $wR_2 = [\Sigma\{w(F_0^2 - F_c^2)^2\}/\Sigma\{w(F_o^2)^2\}^{1/2}$. [c]) $[I > 2\sigma(I)]$

Table 2. *Selected Bond Lengths* [Å] *and Angles* [°] *for* **1** *and* **2a**

	1	**2a**
Rh(1)–O(2)	2.062(2)	2.054(6)
Rh(1)–O(1)	2.072(2)	2.200(6)
Rh(1)–P(2)	2.1961(8)	2.370(2)
Rh(1)–P(1)	2.2083(9)	2.390(2)
Rh(1)–C(3)	–	2.079(8)
Rh(1)–I(1)	–	2.6651(9)
O(2)–N(2)	1.300(4)	1.282(10)
O(1)–N(1)	1.321(4)	1.348(10)
N(2)–N(1)	1.271(4)	1.271(11)
N(1)–C(1)	(A)1.55(2)	1.493(8)
N(1)–C(1)	(B)1.46(2)	–
C(1)–C(2)	(A)1.41(2)	1.468(9)
C(1)–C(2)	(B)1.50(2)	–
O(2)–Rh(1)–O(1)	76.48(10)	76.4(2)
O(2)–Rh(1)–P(2)	94.87(7)	89.1(2)
O(1)–Rh(1)–P(2)	171.35(8)	90.6(2)
O(2)–Rh(1)–P(1)	168.69(7)	89.9(2)
O(1)–Rh(1)–P(1)	92.32(8)	88.5(2)
P(2)–Rh(1)–P(1)	96.34(3)	178.83(8)
N(1)–O(1)–Rh(1)	108.9(2)	104.1(5)
N(2)–O(2)–Rh(1)	115.6(2)	117.1(6)
N(1)–N(2)–O(2)	114.0(3)	115.5(8)
N(2)–N(1)–O(1)	125.0(3)	126.9(7)
N(2)–N(1)–C(1)	(A)122.3(8)	122.2(10)
O(1)–N(1)–C(1)	(A)111.8(8)	110.8(9)
C(2)–C(1)–N(1)	(A)105.0(13)	116.4(13)
N(2)–N(1)–C(1)	(B)113.5(9)	–
O(1)–N(1)–C(1)	(B)120.0(9)	–
N(1)–C(1)–C(2)	(B)100.6(13)	–
O(2)–Rh(1)–I(1)	–	177.5(2)
C(3)–Rh(1)–I(1)	–	92.5(3)
O(1)–Rh(1)–I(1)	–	101.3(2)
P(2)–Rh(1)–I(1)	–	89.90(6)
P(1)–Rh(1)–I(1)	–	91.00(6)
O(2)–Rh(1)–C(3)	–	89.8(3)
O(1)–Rh(1)–C(3)	–	166.2(3)
C(3)–Rh(1)–P(2)	–	89.9(2)
C(3)–Rh(1)–P(1)	–	90.8(2)

diffraction experiment, followed by NMR spectral characterization, gave a spectrum corresponding to the major isomer, **2a**.

3. Discussion. – Diazeniumdiolates have surprisingly variable reactions with different electrophiles, and this variation is further modulated by the nitrogen substituents. For example, protons readily lead to the release of two NO$^{\bullet}$ and a secondary amine when $R_2NN(O)NO^-$ is dissolved in neutral aqueous media (*Eqn. 1*), but the corresponding alkyl and aryl derivatives have markedly greater stability (but not infinitely so!) in this medium. In contrast, many first-row divalent metal ions are chelated by either of these diazeniumdiolates [15–18]. At the outset of this research, second- and third-row transition metal complexes, especially those deficient in

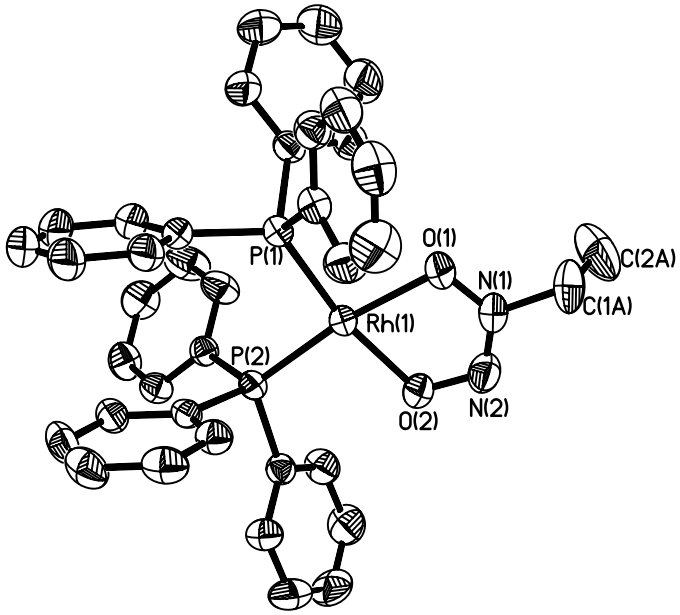

Fig. 1. *ORTEP Plot of the structure of* $Rh(\eta^2\text{-}O_2N_2Et)(PPh_3)_2$ (**1**). H-Atoms are omitted for clarity; only a single ethyl orientation shown.

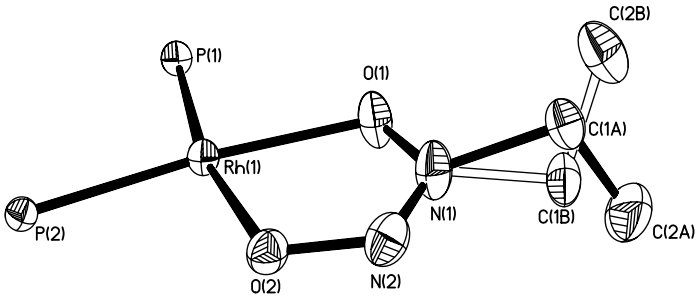

Fig. 2. *ORTEP Representation for the two ethyl geometries in* **1**

electron-accepting ligands such as CO and NO•, seemed ideal candidates to activate the diazeniumdiolate moiety in unusual ways. This is, indeed, the case for the dialkylamino-substituted diazeniumdiolate, which first chelates in a known manner, but then decomposes to give a nitrosyl complex (*Scheme 2*). The other product of this transformation, formally the diethylnitrosamine, Et_2NNO, was not detected spectroscopically in the by-products, and the mechanism for this transformation is not immediately obvious. A possible rationale for why reductive nitrosylation occurs in this case, and in **1**, is that reconfiguration of the chelate, to a possible structure such as **B**, **C**, or **D** might lead to activation of the N(O)NO framework. While **C** might seem the most logical intermediate, the N_β lone pair is remarkably non-nucleophilic [5][6]. The five-member chelate ring shown in **D** would require (*Z*) to (*E*) isomerization of the

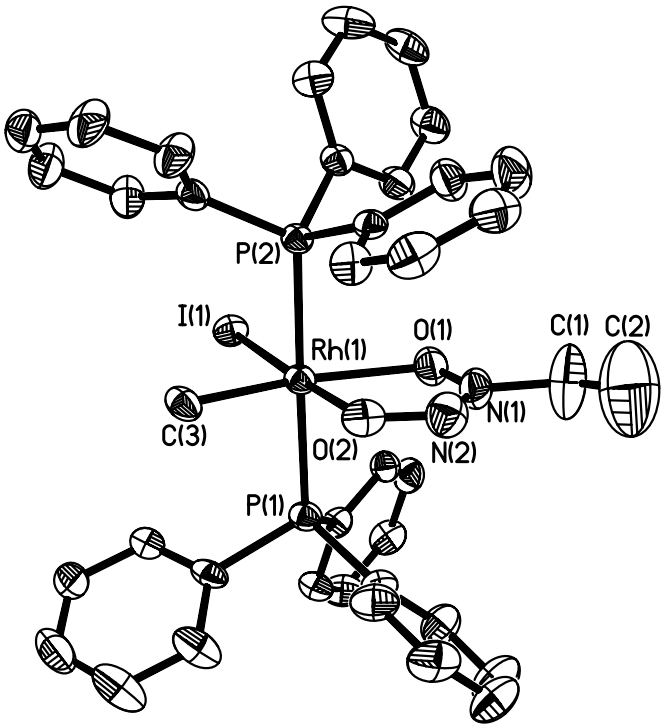

Fig. 3. *ORTEP Plot showing the major isomer of* **2**. H-Atoms are omitted for clarity.

diazenium diolate backbone, and the barriers to this for the uncoordinated ligand appear to be fairly large [1]. Clearly, further product identification is required as a first step to unravel these mechanistic issues.

$$R_2NN(O)NO^- + H^+ \rightarrow R_2NH + 2\ NO \qquad (1)$$

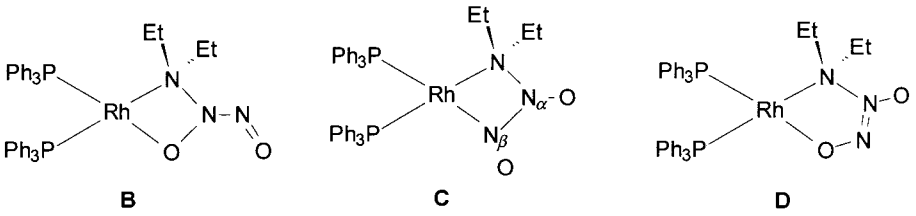

The reductive nitrosylation shown in *Scheme 2* is a formal two electron change in oxidation state for the metal, from Rh^{I} to Rh^{-I}. Other well-known reductive nitrosylation reactions (*cf.*, *Eqn. 2*) [19] couple the metal's reduction to a formal change in oxidation state of nitrogen. Thus, the chief distinctions between the reactions in *Scheme 2* and *Eqn. 2* are, first, the formal change in the metal's oxidation state being

two and one electrons, respectively, and, second, the nature of the coupling of the change in formal oxidation state for the metal and nitrogen.

$$Fe(TPP)Cl + 2\,NO + MeO^- \rightarrow Fe(TPP)(NO) + MeONO + Cl^- \qquad (2)$$

The structural results illustrate trends typical of Rh^I and Rh^{III} complexes: shorter $Rh-PPh_3$ bond lengths for **1** than found for **2a**, and Rh geometries representative of square-planar bis[triphenylphosphine]Rh^I centers. The most significant structural change observed in the ethyldiazeniumdiolate ligand upon oxidative addition of MeI to Rh is the pronounced lengthening of the Rh–O(1) bond to 2.200(6) Å, for the O-atom *trans* to the Me group in **2a**. This almost certainly reflects the strong *trans* influence of the Me group [20]. Unfortunately, the typically large esd's for the remaining structural parameters for the ethyldiazeniumdiolate preclude additional structural interpretation of the effect that diminished Rh–O(1) interaction has on the remainder of the ligand. This effect has been theoretically and experimentally examined in some detail for nonchelating counterions [1]. The structural reorganization upon oxidative addition of MeI, that is, *cis*- to *trans*-triphenylphosphine geometries, and the pair of isomers observed, are in keeping with known trends in this reaction [21][22].

Experimental Part

General. Instrumentation and standard methods have been described in prior reports [6]; all manipulations of solns. of the Rh^I complexes were performed in an inert-atmosphere box. $RhCl(PPh_3)_3$ [23], K[EtN(O)NO] [24], $[Et_2NH_2][Et_2NN(O)NO]$ [25] were prepared by lit. methods. IR Spectra: $\tilde{\nu}$ in cm^{-1}. NMR Spectra: δ in ppm, J in Hz.

$Rh(\eta^2\text{-}O_2N_2Et)(PPh_3)_2$ (**1**). To a dark red soln. of $RhCl(PPh_3)_3$ (103.5 mg, 0.1 mmol) in CH_2Cl_2 (15 ml) was added a clear soln. of [K][EtNONO] (29.3 mg 0.2 mmol) in MeOH (10 ml). Immediately after both solns. were combined, a color change from dark red to light orange occurred. The soln. was then stirred for 2 h at r.t., and the soln. stripped of solvent under vacuum. Recrystallization of the resulting orange powder from CH_2Cl_2/MeOH gave 57.0 mg, 0.1 mmol (71%) of **1** isolated as orange blocks. Crystals suitable for X-ray diffraction were grown by vapor-phase diffusion of EtOH into a CH_2Cl_2 soln. of $Rh(\eta^2\text{-}O_2N_2Et)(PPh_3)_2$. IR (KBr): 1340*m*, 1307*m*, 1264*m*, 1243*m*, 914*s* (EtNONO). ^{1}H-NMR ($CDCl_3$): 3.51 (*q*, ^3J(H,H) = 7.4, CH_2); 0.77 (*t*, ^3J(H,H) = 7.1, Me). ^{31}P-NMR (CD_2Cl_2): 55.5, 53.4 (doubled AB *q*, $^2J(P_a,P_b) = 56.4$, $^1J(P_a,Rh) = 194.5$, $^1J(P_bRh) = 189.2$). Anal. calc. for $RhP_2C_{38}N_2O_2H_{35}$: C 63.70, N 3.91, H 4.92; found: C 63.75, N 3.84, H 4.94.

$Rh(I)(Me)(\eta^2\text{-}O_2N_2Et)(PPh_3)_2$ (**2a**,**b**). Compound **1** (90 mg, 0.12 mmol) in 10 ml CH_2Cl_2 was treated with MeI (0.078 ml, 0.12 mmol), and the resulting mixture stirred for 2 h, during which time the color changed from a light orange to brown-red. Addition of MeOH and concentration gave 88 mg (85% yield) of brown-red solid, which corresponds to a 5:1 ratio of major to minor geometric isomers (see *Discussion*). The crystal for the structural characterization was grown by vapor-phase diffusion of EtOH into a CH_2Cl_2 soln. of Rh(Me)(I)(EtNONO)$(PPh_3)_2$. IR (KBr): 1335*w*, 1303*m*, 1263*w*, 1232*w*, 919*m* (EtNONO). ^{1}H-NMR (CD_2Cl_2, major species): 3.02 (*q*, ^3J(H,H) = 7.1, CH_2); 1.46 (*dt*, ^3J(P,H) = 3.9, ^2J(Rh,H) = 2.3, RhMe); 0.78 (*t*, ^3J(H,H) = 7.2, CH_2*Me*); (minor species): 2.23 (*q*, ^3J(H,H) = 7.2, CH_2); 1.31 (*dt*, ^3J(P,H) = 5.9, ^2J(Rh,H) = 3.0, RhMe); 0.42 (*t*, ^3J(H,H) = 7.3, CH_2*Me*). ^{31}P-NMR (CD_2Cl_2, major species): 19.64 (*d*, ^2J(P,Rh) = 106.6); (minor species): 20.65 (*d*, ^2J(P,Rh) = 105.1). Anal. calc. for $RhP_2IC_{39}N_2O_2H_{38}\cdot 0.25\ CH_2Cl_2$: C 53.58, N 3.18, H 4.41; found: C 53.55, N 3.25, H 4.44.

Reaction of $RhCl(PPh_3)_3$ and $[Et_2NNONO][Et_2NH_2]$. A soln. of $[Et_2NH_2][Et_2NN_2O_2]$ (11.4 mg, 0.055 mmol) in CD_3OD (0.05 ml) was added to a soln. of $RhCl(PPh_3)_3$ (25.0 mg 0.027 mmol) in C_6D_6 (1 ml). The red suspension immediately turned into a yellow soln. The soln. was transferred to an NMR tube under N_2 and immediately examined by NMR spectroscopy. After 2 h, the solns. were recombined and dried under vacuum to give a yellow solid. Further purification by recrystallization from CH_2Cl_2 and MeOH afforded 14.2 mg of an impure yellow powder product. IR (KBr): 1610 (NO).

X-Ray Crystallography. X-Ray diffraction data for **1** and **2a** were collected on a *Siemens P4* diffractometer equipped with a molybdenum tube and graphite monochromator at 25°, $\lambda = 0.71073$ Å[1]). Crystals were mounted on a glass fiber with epoxy resin, and the unit-cell dimensions were determined from *ca.* 40 accurately centered reflections in high 2θ angles with the XSCANS program [26]. Data were collected in ω scan modes, and three standard reflections, measured after every 97th reflection, exhibited no significant loss of intensity in either data collection. Before soln. and refinement the data were corrected for *Lorentz*-polarization effects and absorption, the structures were solved by direct methods and refined by least-squares techniques with adaptation of the full-matrix weighted least-squares on F^2 with the SHELXTL program [27]. Additional details of the data collection parameters and refinement are collected in *Table 1*, and important structural parameters are collected in *Table 2*. In both cases, all non-H-atoms were refined anisotropically. H-Atoms were placed in calculated positions and refined isotropically. In the case of **1**, the two C-atoms of the $EtN_2O_2^-$ moiety exhibited high thermal parameters during the initial stages of refinement, indicating positional disorder, which was finally modeled over two positions as shown in *Fig. 2.*

The authors gratefully acknowledge financial support for this research from the *NIH* (P20 RR1553), from the *Air Force Office of Scientific Research* (F 49620-96-1-0417 and 98-1-0461), and from the *DOE* (Grant DE-FCO2-91ER).

REFERENCES

[1] L. K. Keefer, J. L. Flippen-Anderson, C. George, G. M. Sheldrick, T. M. Dunams, D. Christodoulou, J. E. Saavedra, E. S. Sagan, D. S. Bohle, *Nitric Oxide: Biology and Chemistry* **2001**, *5*, 377.
[2] C. Coronelli, C. R. Pasqualucci, G. Tamoni, G. G. Gallo, *Farmaco. Ed. Sci*. **1966**, *21*, 269.
[3] S. R. Fletcher, A. Shortland, A. C. Skapski, G. Wilkinson, *J. Chem. Soc., Chem. Commun*. **1972**, 922.
[4] J. Sand, F. Singer, *Justus Liebigs Ann. Chem*. **1903**, *329*, 190.
[5] R. B. Woodward, C. Wintner, *Tetrahedron Lett*. **1969**, 2689.
[6] N. Arulsamy, D. S. Bohle, J. A. Imonigie, E. S. Sagan, *J. Am. Chem. Soc*. **2000**, *122*, 5539.
[7] K. M. Davies, D. A. Wink, J. E. Saavedra, L. K. Keefer, *J. Am. Chem. Soc*. **2001**, *123*, 5473.
[8] J. Reglinski, D. R. Armstrong, K. Sealy, M. D. Spicer, *Inorg. Chem*. **1999**, *38*, 733.
[9] S. S. Basson, J. G. Leipoldt, W. Purcell, J. A. Venter, *Acta Crystallogr., Sect. C* **1992**, *48*, 171.
[10] S. S. Basson, J. G. Leipoldt, A. Roodt, J. A. Venter, *Inorg. Chim. Acta* **1986**, *118*, L45.
[11] S. S. Basson, J. G. Leipoldt, A. Roodt, J. A. Venter, *Inorg. Chim. Acta* **1987**, *31*, 31.
[12] S. S. Basson, J. G. Leipoldt, J. A. Venter, *Acta Crystallogr., Sect. C* **1990**, *46*, 1324.
[13] K. G. Caulton, *Inorg. Chem*. **1974**, *13*, 1774.
[14] J. P. Collman, N. W. Hoffman, D. E. Morris, *J. Am. Chem. Soc*. **1969**, *91*.
[15] D. Christodoulou, C. George, L. K. Keefer, *J. Chem. Soc., Chem. Commun*. **1993**, 937.
[16] J. Charalambous, L. I. B. Haines, N. J. Harris, F. B. Henrick, F. B. Taylor, *J. Chem. Res.* **1984**, *220*, 2101.
[17] J. L. Schneider, V. G. Young, W. B. Tolman, *Inorg. Chem*. **1996**, *35*, 5410.
[18] P. L. Piciulo, W. R. Scheidt, *Inorg. Nucl. Chem. Lett*. **1975**, *11*, 309.
[19] D. S. Bohle, C.-H. Hung, *J. Am. Chem. Soc*. **1995**, *117*, 9584.
[20] L. M. Venanzi, *Chem. Br.* **1968**, *4*, 162.
[21] J. Halpern, *Acc. Chem. Res.* **1970**, *3*, 386.
[22] J. K. Stille, K. S. Y. Lau, *Acc. Chem. Res.* **1977**, *10*, 434.
[23] J. A. Osborn, F. H. Jardine, F. H. Young, G. Wilkinson, *J. Chem. Soc. A* **1966**, 171.
[24] *Badische Anilin- u. Soda-Fabrik A.G.*, German Pat. 815,537, *Chem. Abs.* **1960**, *54*, 3270.
[25] R. S. Drago, F. E. Paulik, *J. Am. Chem. Soc*. **1960**, *82*, 9698.
[26] XSCANS 2.21, *Siemens Energy and Automation, Inc.*, 1993.
[27] SHELXTL Crystallographic System 5.4, *Siemens Analytical X-Ray Instruments, Inc.*, 1996.

Received September 7, 2001

---

[1]) Crystallographic data (excluding structure factors) for the structures reported in this paper have been deposited with the *Cambridge Crystallographic Data Centre* as Deposition No. CCDC 169860 and 169861. Copies of the data can be obtained, free of charge, by writing to the CCDC, 12 Union Road, Cambridge CB2 1EZ, UK (fax: +44(1223)336066; e-mail: deposit@ccdc.com.ac.uk).